



Normal bone marrow signal characteristics in whole-body diffusion-weighted images of amateur marathon runners

Hongwei Cao¹^, Fengzhen Cui¹, Hong Yu¹, Jianling Cui¹, Feilong Ma², Lisha Duan¹

¹Department of Radiology, The Third Hospital of Hebei Medical University, Shijiazhuang, China; ²Department of Radiology, Affiliated Hospital of Chengde Medical University, Chengde, China

Contributions: (I) Conception and design: H Cao, J Cui; (II) Administrative support: J Cui; (III) Provision of study materials or patients: H Cao, F Cui, J Cui; (IV) Collection and assembly of data: H Cao, H Yu, L Duan; (V) Data analysis and interpretation: H Cao, H Yu, L Duan; (VI) Manuscript writing: All authors; (VII) Final approval of manuscript: All authors.

Correspondence to: Jianling Cui, MD, PhD. Department of Radiology, The Third Hospital of Hebei Medical University, No. 139 Ziqiang Road, Shijiazhuang 050051, China. Email: jianlingcui@hebmh.edu.cn.

Background: Marathon training can reverse bone marrow conversion; however, little is known about the normal bone marrow whole-body diffusion-weighted imaging (WB-DWI) signal characteristics of amateur marathon runners. If marathon training can cause diffuse hyperintensity of bone marrow on WB-DWI is essential for correctly interpreting the diffusion-weighted (DW) images. This study sought to evaluate the WB-DWI signal characteristics of normal bone marrow in amateur marathon runners.

Methods: In this prospective cross-sectional study, 30 amateur marathon runners who had trained for over 3 years for regular or half-marathon races and had a running frequency of more than 20 days a month at a distance of more than 100 km per month from the Chengde Marathon Outdoor Sports Association in Hebei, China, and 30 age- and gender-matched, healthy volunteers (the control group) who had no long-term heavy-load sports history were recruited between April 2021 to September 2021. All the subjects underwent WB-DWI (b -value: 0, 800 s/mm²) and lumbar vertebral transverse relaxation time (T2) mapping. The bone marrow WB-DWI signal characteristics were analyzed visually and statistically by chi-square (χ^2) tests. The apparent diffusion coefficient (ADC), DWI signal intensity, and T2 values of the bone marrow were quantitatively and statistically analyzed by the independent sample t -test and Mann-Whitney U test.

Results: No subjects were excluded from the study. The bone marrow of 30 of the 60 subjects (aged 30–50 years) showed diffuse hyperintensity in the DW images. However, in all 60 subjects, the humeral heads, femoral heads, and great trochanters had low signals. The frequency of diffuse bone marrow DWI hyperintensity was significantly higher in the male amateur marathon runners (50%) than the male controls (5%, $P=0.003$), but no such significant difference was found between the female amateur marathon runners (100%) and female controls (90%, $P>0.99$). The DW signal intensity ratios of bone marrow to muscle ($SIR_{BM-muscle}$) were significantly higher in the male amateur marathon runners than the male controls in the thoracic vertebrae (4.68 vs. 3.57, $P=0.021$), lumbar vertebrae (4.49 vs. 3.01, $P<0.001$), sacrum (3.67 vs. 2.62, $P=0.002$), and hip (3.45 vs. 2.50, $P=0.002$), but were only significantly higher in the female amateur marathon runners than the female controls in the thoracic vertebrae (7.69 vs. 5.87, $P=0.029$) and hip (4.76 vs. 3.92, $P=0.004$). The mean T2 values of the lumbar vertebrae were significantly higher in the male amateur marathon runners than the male controls (116.76 vs. 97.63 ms, $P=0.001$), but no such significant difference was observed between the female amateur marathon runners and the corresponding controls (118.58 vs. 124.10 ms, $P=0.386$).

^ ORCID: 0000-0002-3247-6893.

Conclusions: Marathon training resulted in diffuse hyperintensity in the bone marrow based on WB-DWI in 50% of the male amateur marathon runners aged 30–50 years. Thus, when WB-DWI is used for bone marrow disease screening, marathon training history should be considered to avoid false-positive diagnoses.

Keywords: Bone marrow; magnetic resonance imaging (MRI); whole-body diffusion-weighted imaging (WB-DWI); amateur marathon runners

Submitted Jul 16, 2023. Accepted for publication Jan 11, 2024. Published online Mar 07 2024.

doi: 10.21037/qims-23-1006

View this article at: <https://dx.doi.org/10.21037/qims-23-1006>

Introduction

In the literature, the sensitivity of whole-body diffusion-weighted imaging (WB-DWI) (1) for detecting bone marrow infiltrating diseases is higher than that of conventional magnetic resonance imaging (MRI) and bone scintigraphy, and at least equivalent to that of fluorine-18-fluorodeoxy-glucose positron emission tomography (2-5). Thus, in terms of functional imaging, WB-DWI is a good method for screening bone marrow infiltrating lesions [e.g., multiple myeloma (MM), bone marrow metastasis, leukemia, and lymphoma] (6-9), as it has no radiation and high sensitivity (10-12). Many cancers, such as breast cancer and lung cancer, are prone to bone metastasis. In 2020, breast cancer and lung cancer were the first (11.7%) and second (11.4%) most commonly diagnosed cancers worldwide (13). Among individuals newly diagnosed with advanced breast cancer, 50% have bone metastases (14), and about 17–43.8% of women patients with breast cancer are diagnosed before the age of 50 years (15,16). Very little research has been conducted on breast cancer and lung cancer patients with diffuse bone marrow infiltration (17-19). Approximately 10% of MM patients are diagnosed when they are aged less than 50 years old, and 25% of MM patients present with diffuse bone marrow infiltration (20,21). About 10–20% of leukemia patients are aged 30–50 years old at the time of onset (22), and a portion of leukemia patients show diffuse bone marrow infiltration (19,23). After the diagnosis and treatment of the above-mentioned cancers, regular screening for bone marrow lesions is required (10,11). Some people aged 30–50 years, including early-onset cancer patients after surgery, engage in marathon, or long-distance running for exercise (24).

WB-DWI is an important method for predicting tumor responses to therapy in the Myeloma Response Assessment and Diagnosis System (10). In any pathologic process, including focal or diffuse infiltration, increased signal

intensity on diffusion-weighted imaging (DWI) indicates the replacement of the normal bone marrow (21,25-27). However, not all diffuse hyperintensities in the high *b*-value diffusion-weighted (DW) images of bone marrow indicate lesions; normal bone marrow can also display diffuse hyperintensity, which indicates a higher portion of red bone marrow (28,29). Ording Müller *et al.* (30) visually evaluated the WB-DWI ($b=1,000 \text{ s/mm}^2$) signal features of bone marrow in the normal lumbar spines and pelvises of 42 children (24 male and 18 female; age range, 2 months to 16 years) and found diffuse high signal intensities in both the vertebral bodies and pelvic skeletons of all the children. In a previous assessment of the bone marrow DW signal intensities of 98 healthy volunteers aged 21–81 years based on WB-DWI (31), diffuse bone marrow signal hyperintensity was more common in Chinese females aged 21–50 years (68.4%) than those aged 51–81 years (15.4%). Further research indicated that the proportion of DWI bone marrow hyperintensity was significantly higher in premenopausal (91%) women than perimenopausal (75%) and postmenopausal (8%) women (32).

Numerous studies have shown that high altitude (33), the use of granulocyte colony-stimulating factors (10,34), chronic anemia (29), and heavy smoking can stimulate marrow hyperplasia (21,35), which also produces DWI hyperintensities. Aerobic training, such as marathon training, can reverse bone marrow conversion, which manifests as focal or diffuse hypointense regions on the T1-weighted sequence, and hyperintensity in the corresponding region on the fat-suppressed T2-weighted sequence (36-38). However, the WB-DWI signal characteristics of bone marrow in marathon runners had not previously been examined.

We hypothesized that marathon running would cause diffuse hyperintensity of bone marrow on WB-DWI. In this study, we compared the bone marrow DWI signal characteristics of normal adult amateur marathon runners

with those of healthy volunteers who did not engage in any heavy-load training. The results provide valuable reference information for the screening of whole-body bone marrow diseases using WB-DWI. We present this article in accordance with the STROBE reporting checklist (available at <https://qims.amegroups.com/article/view/10.21037/qims-23-1006/rc>).

Methods

Subject selection

This prospective study was conducted in accordance with the Declaration of Helsinki (as revised in 2013) and was approved by the Ethics Committee of The Third Hospital of Hebei Medical University. All the participants included in this study signed an informed consent form before undergoing the MRI examination.

Amateur marathon runners were randomly recruited from the Chengde Marathon Outdoor Sports Association in Hebei, China, from April 2021 to September 2021. Amateur marathon runners were defined as those who had not participated in formal training as occupational runners (39). To be eligible for inclusion in this study, the amateur marathon runners had to meet the following inclusion criteria: (I) have engaged in over 3 years of training for regular or half-marathon races; (II) have a running frequency of more than 20 days a month with a distance of more than 100 km per month; and (III) meet the common inclusion criteria for the two groups.

The age- and gender-matched healthy volunteers were recruited from friends and colleagues as controls during the same period. To be eligible for inclusion in this study, the controls had to meet the following inclusion criteria: (I) have never participated in any marathon activities or other long-term heavy-load sports (e.g., swimming, cycling, and aerobics); and (II) meet the common inclusion criteria for the two groups.

The common inclusion criteria for the two groups were as follows: (I) normal blood routine laboratory examination results; (II) no known clinical or imaging evidence of any bone disease (e.g., tumors, metastases, and metabolic disorders); (III) no history of hormone and granulocyte colony-stimulating factor use (34); (IV) no history of heavy smoking (≥ 20 cigarettes per day) or obesity [body mass index (BMI) ≥ 28 kg/m²] (40); (V) regular menstruation for female volunteers; and (VI) no contraindication to the MRI examination.

The exclusion criteria for the two groups were as follows: (I) Modic changes involving more than half of the vertebral body; and/or (II) suboptimal image quality.

Based on the above criteria, 30 amateur marathon runners (20 males and 10 females, aged 30–50 years) were recruited in the amateur marathon runners group. Of them, one male amateur marathon runner had a history of lumbar vertebrae minor trauma 20 years ago, which presented normally in the current MRI, one male amateur marathon runner had a history of a cruciate ligament tear 20 years ago, and another had a history of a medial collateral ligament 5 years ago in the right knee, which fell outside the scope of the WB-DWI in this study. Thirty healthy volunteers (20 males and 10 females) were recruited as controls. No subjects were excluded from the study.

The following clinical information was recorded for each subject: age, sex, BMI [defined as BMI = weight (kg)/height (m)²], white blood cell count (WBC, 10⁹/L), red blood cell count (RBC, 10¹²/L), platelet count (PLT, 10⁹/L), hemoglobin (HGB, g/L), and red blood cell distribution width-coefficient of variation (RDW-CV, %).

MRI examination

MRI was performed using a 1.5-Tesla scanner (Magnetom Avanto, Siemens, Erlangen, Germany) equipped with a 12-element head matrix coil, a four-element neck matrix coil, a 24-element spine matrix coil, and four six-element body matrix coils. The parameters of the DWI sequence were as follows: repetition time/echo time (TR/TE), 8,000/83 ms; field of view (FOV), 50×50 cm²; slice/gap, 4/0 mm; matrix, 192×148; number of excitation (NEX), 6; and *b*-values, 0 and 800 s/mm². The chemical shift selective saturation technique was used in the DWI sequence for fat suppression. Axial slices were acquired from the head to the middle femur using the 4–5 station approach. Coronal maximal intensity projections of the DW images were reconstructed using the original axial images and the inverted images for background suppression. Quantitative apparent diffusion coefficient (ADC) maps were calculated by two *b* values, 0 and 800 s/mm², automatically generated by the MRI system for measurement.

T2 values were measured by a multi-echo spin-echo sequence and calculated with an exponential decay model. The parameters of the T2 mapping sequence for the lumbar spine were as follows: TR, 2,000 ms; TE, 10.4/20.8/31.2/41.6/52.0/62.4 ms; slice/gap, 4/0.8 mm; FOV, 25×24 cm²; matrix, 256×174; and NEX, 2.

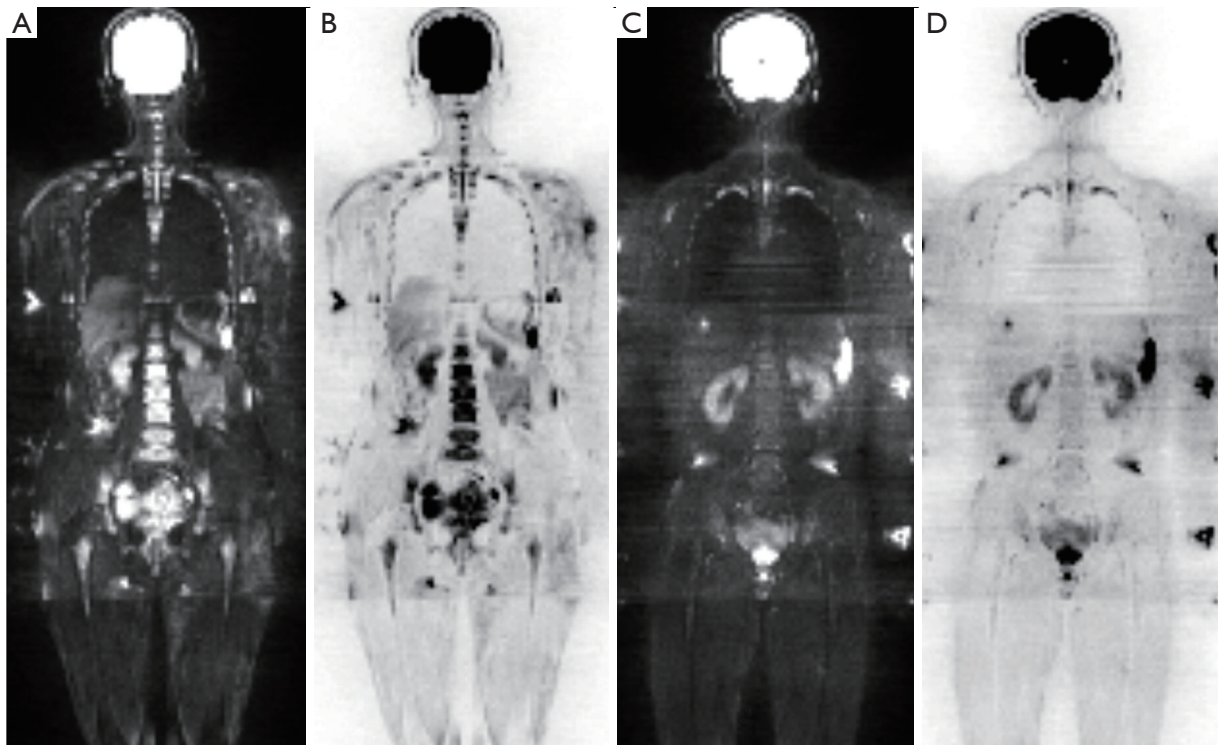


Figure 1 Visual evaluation criteria for defining hyperintensity and hypointensity of bone marrow on WB-DW images ($b=800 \text{ s/mm}^2$). (A,C) WB-DW images; (B,D) inverted images. Diffuse hyperintensity of bone marrow in WB-DW images was defined as those signals that were higher than the signals of muscles (A,B); diffuse hypointensity of bone marrow in WB-DW images was defined as those signals that were lower than or equal to the signals of muscles (C,D). WB-DW, whole-body diffusion-weighted.

Visual evaluation of bone marrow WB-DWI signal intensity

The signal intensity of the bone marrow on the DW images (b -value of 800 s/mm^2) was visually evaluated independently by two radiologists (H.C. and Yongzhong Chen, MD, with 15 and 3 years of clinical experience interpreting musculoskeletal MRI scans, respectively) using the same criteria. Bone marrow signal hyperintensity (Figure 1A,1B) was defined as an intensity higher than that of the surrounding muscles, while hypointensity (Figure 1C,1D) was defined as an intensity lower than or equal to that of the surrounding muscles (31,32). To assess the intra-observer agreement, H.C. re-evaluated the DW images for all participants following the procedure used in the first evaluation one month later without knowledge of the results of the first reading.

Quantitative image analysis

The signal intensity of the bone marrow (SI_{BM}) and

surrounding muscles (SI_{muscle}) in the DW images (b -value = 800 s/mm^2) was measured on the workstation. A circular or elliptical region of interest (ROI) was drawn manually on the DW images ($1.5\text{--}2.5 \text{ cm}^2$; as large as possible, while avoiding the basivertebral vessels, cortex, and artifacts) and then automatically copied onto the corresponding ADC map (Figure 2); the ADC values of the ROIs were read from the screen directly. In the muscles, the ROIs ($1.5\text{--}2.5 \text{ cm}^2$) were placed on the erector spinae and multifidus muscle for the thoracolumbar vertebrae and the gluteal muscle for the sacrum and hip (Figure 2A). In the thoracolumbar vertebrae, one ROI was placed by identifying a central slice in each of the five thoracic vertebrae (T8 through T12) and each of the five lumbar vertebrae (L1 through L5). In the sacrum, ROIs were placed on five consecutive slices with the maximum area of the cancellous bone. In the hip, ROIs were placed on five slices of the sacroiliac joint and symphysis pubis level of each side with the maximum area of the cancellous bone. The ROIs of the same part were the same to the greatest

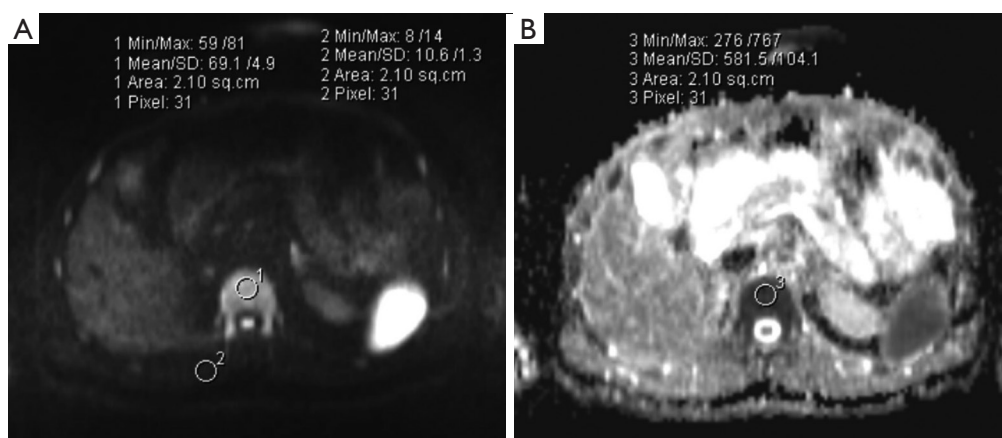


Figure 2 A schematic diagram showing the drawing of the ROI. (A) ROI 1 for SI_{BM} and ROI 2 for SI_{muscle} were manually drawn on the axial DW image ($b=800$ s/mm²). (B) ROI 1 in the DW image was automatically copied onto the corresponding ADC map, and defined as ROI 3. SD, standard deviation; ROI, region of interest; SI_{BM} , signal intensity of bone marrow; SI_{muscle} , signal intensity of muscle; DW, diffusion-weighted; ADC, apparent diffusion coefficient.

extent possible. The average measurements of five vertebrae bodies or slices were used for further analysis.

To measure the T2 value of the lumbar vertebrae, a circular ROI (2.0 cm²) was manually drawn at the center of the first to the fifth vertebral body (L1–L5) on the middle sagittal T2 mapping images. The average T2 values of the five vertebrae bodies were used for further analysis.

For inter-observer reliability testing, the SI_{BM} , SI_{muscle} , ADC, and T2 values were measured by H.C. and Yongzhong Chen, MD using the same criteria. One month later, to test the intra-observer reliability, the measurements were repeated by H.C. using the same methods as above without reference to the previously determined values. Only the H.C. measurements were used for the overall statistical analysis (29).

The DW $SIR_{BM-muscle}$ was defined as (10,29,41):

$$SIR_{BM-muscle} = SI_{BM} / SI_{muscle} \quad [1]$$

Statistical analysis

All the statistical analyses were performed using commercial SPSS 22.0 software (SPSS Inc., Chicago, IL, USA). All the tests were two-sided with a significance level of $P < 0.05$. The chi-square (χ^2) test was used to compare the frequency of hyperintense bone marrow in the DW images between each group. Fisher's exact test was used if the sample size was less than 40.

To compare the differences in the $SIR_{BM-muscle}$, ADC, and T2 values between the amateur marathon runner and control groups, the independent sample *t*-test and Mann-Whitney *U* test were used for normally and non-normally distributed data, respectively.

Intra- and inter-observer agreement for the visual assessment of the bone marrow signal intensity in the DW images was analyzed using the *k* statistic suggested by Laborie *et al.* (42) and adapted from Landis and Koch in 1977 (43). The *k* values were interpreted as follows: $k=0-0.20$, poor agreement; $k=0.21-0.40$, fair agreement; $k=0.41-0.60$, moderate agreement; $k=0.61-0.80$, good agreement; and $k=0.81-1.00$, very good agreement.

The intra- and inter-observer reliability for the SI_{BM} , SI_{muscle} , ADC, and T2 measurements was determined based on the intraclass correlation coefficient (ICC). The ICC values were interpreted as follows: 0.41–0.60, moderate reliability; 0.61–0.80, good reliability; and ≥ 0.81 , very good reliability (31,44).

Results

Subject demographics

The demographic characteristics of the amateur marathon runner and control groups are set out in *Table 1*. The mean age, BMI, WBC, RDW-CV, PLT, RBC, and HGB did not differ significantly between the two groups (all $P > 0.05$).

Table 1 Demographic characteristics of the amateur marathon runners and controls

Characteristic	Controls (n=30)	Amateur marathon runners (n=30)	P value
Age (years)	38.43±5.78	40.73±5.91	0.133
BMI (kg/m ²)	24.37±3.26	23.01±2.01	0.057
WBC (10 ⁹ /L)	6.27±2.04	6.38±1.22	0.801
RDW-CV (%)	12.78 (12.10, 13.10)	12.95 (12.48, 13.63)	0.081
PLT (10 ⁹ /L)	234.02±46.66	211.15±52.77	0.081
RBC (10 ¹² /L)	4.65±0.52	4.67±0.33	0.809
HGB (g/L)	144.50 (132.00, 153.25)	142.50 (134.50, 151.78)	0.745

Data are presented as the mean ± standard deviation, or median (M) and quartile (Q1, Q3). BMI, body mass index; WBC, white blood cell; RDW-CV, red blood cell distribution width-coefficient of variation; PLT, platelet; RBC, red blood cell; HGB, hemoglobin.

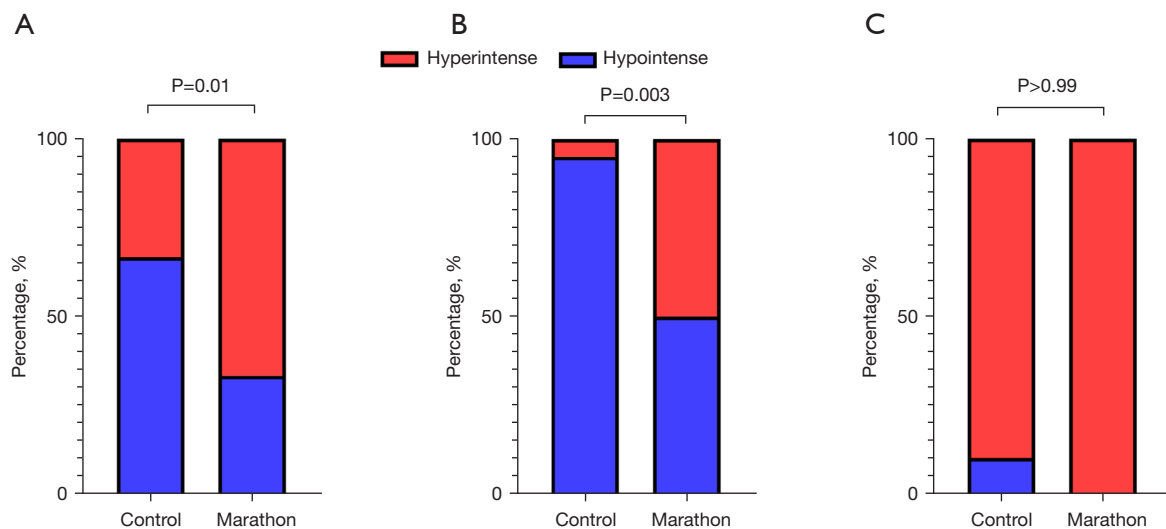


Figure 3 Stacked bar chart comparing the frequency of diffuse hyperintensity of the bone marrow on DW images ($b=800 \text{ s/mm}^2$) between the amateur marathon runners and controls. (A) All subjects; (B) male subjects; (C) female subjects. DW, diffusion-weighted.

Visualization of bone marrow signal intensity in DW images ($b=800 \text{ s/mm}^2$)

The frequency of bone marrow DWI hyperintense signals was significantly higher in the amateur marathon runners [66.67% (20/30)] than the controls [33.33% (10/30); $P=0.01$, *Figure 3A*]. Meanwhile, the frequency was significantly higher in the male amateur marathon runners [50% (10/20)] than the male controls [5% (1/20), $P=0.003$, *Figure 3B*]. However, no statistically significant difference was observed in the frequency of DWI hyperintense signals between the female amateur marathon runners [100% (10/10)] and the female controls [90% (9/10), $P>0.99$, *Figure 3C*].

The bone marrow of 30 of the 60 participants showed diffuse DWI hyperintensity, and all the 60 subjects' humeral heads, femoral heads, and great trochanters showed hypointensity (*Figure 4*). The frequency of diffuse hyperintensity in the metaphysis and proximal humerus was 60% (6/10) in the female amateur marathon runners compared to 40% (4/10) in the female controls, while that in the male amateur marathon runners was 10% (2/20) compared to 0% (0/20) in the male controls, but the difference was not significant ($P=0.656$ and 0.487 , respectively). In the metaphysis and proximal femur, the frequency of diffuse hyperintensity was significantly higher in both the female amateur marathon runners [100%

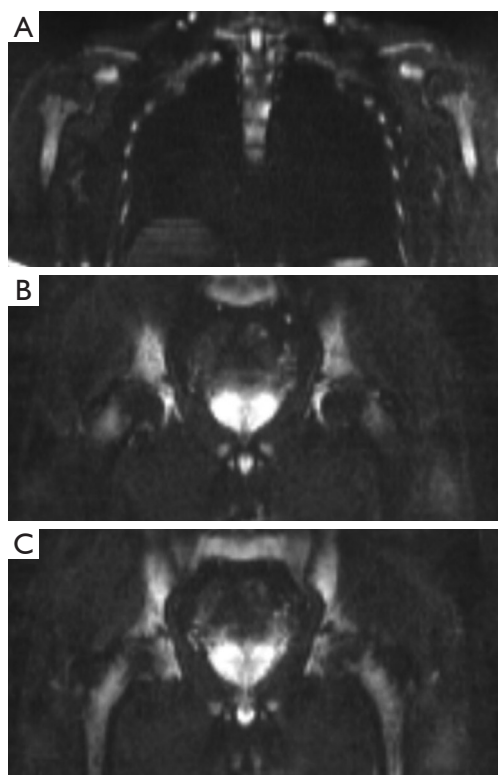


Figure 4 The maximal intensity projection image of the WB-DWI ($b=800$ s/mm²) of a 48-year-old male amateur marathon runner. The bone marrow in the bilateral humeral head (A), femoral head and great trochanter (B,C) was hypointense, while the bone marrow in the metaphysis and proximal of the humerus (A) and femur (B,C) was hyperintense. WB-DWI, whole-body diffusion-weighted imaging.

(10/10)] than the female controls [50% (5/10), $P=0.033$], and the male amateur marathon runners [30% (6/20)] than the male controls [0% (0/20), $P=0.027$].

Bone marrow DWI signal intensity and ADC and T2 measurements

The $SIR_{BM-muscle}$ values were significantly higher in the male amateur marathon runners than the male controls in the thoracic vertebrae (4.68 vs. 3.57, $P=0.021$), lumbar vertebrae (4.49 vs. 3.01, $P<0.001$), sacrum (3.67 vs. 2.62, $P=0.002$), and hip (3.45 vs. 2.50, $P=0.002$); however, the $SIR_{BM-muscle}$ values were only significantly higher in the female amateur marathon runners than the female controls in thoracic vertebrae (7.69 vs. 5.87, $P=0.029$) and hip (4.76 vs. 3.92, $P=0.004$) (see *Table 2*).

The mean T2 values of the lumbar vertebrae were significantly higher in the amateur marathon runners than the controls [116.96 (105.18, 125.51) vs. 106.41 (90.52, 121.41) ms, $P=0.041$]. The mean T2 values of the lumbar vertebrae were significantly higher in the male amateur marathon runners than the male controls [116.76 (104.89, 124.24) vs. 97.63 (89.37, 107.91) ms, $P=0.001$]. The mean T2 values of lumbar vertebrae were not significantly different between the female amateur marathon runners and the corresponding controls (118.58±15.02 vs. 124.10±12.68 ms, $P=0.386$).

The mean ADC of the hip was significantly higher in the amateur marathon runners than the controls (592.69×10^{-6} vs. 525.02×10^{-6} mm²/s, $P=0.002$); however, the ADCs of the other sites did not differ significantly between the two groups ($P>0.05$). The mean ADCs of the sacrum (569.89×10^{-6} vs. 523.81×10^{-6} mm²/s, $P=0.03$) and hip (577.36×10^{-6} vs. 481.16×10^{-6} mm²/s, $P<0.001$) were significantly higher in the male amateur marathon runners than the male controls; however, the ADCs of the other sites did not differ significantly between the male amateur marathon runners and the male controls ($P>0.05$). In terms of the thoracic vertebrae, lumbar vertebrae, sacrum, and hip, the mean ADCs did not differ significantly between the female amateur marathon runners and the female controls ($P>0.05$) (see *Table 3*).

The mean age, BMI, yearly running distance, running years, WBC, RDW-CV, PLT, RBC, and HGB in the male amateur marathon runners with bone marrow hypointensity (10 subjects) did not differ significantly from those with hyperintensity (10 subjects) (see *Table 4*).

Intra- and inter-observer agreement for visual evaluation of the signal intensity of the DW images

The inter-observer agreement ($k=0.900$) and intra-observer agreement ($k=0.833$) were very good for the visual evaluation of DWI signal intensity.

Intra- and interobserver reliability of the quantitative measurements

In the quantitative ROI assessments, the inter-observer reliability between the two investigators for the SI_{BM} , SI_{muscle} , ADC, and T2 measurements ranged from good to very good {ICC =0.969 [95% confidence interval (CI): 0.953–0.978], 0.799 (95% CI: 0.735–0.848), 0.889 (95%

Table 2 Comparison of the SIR_{BM-muscle} values of bone marrow between the amateur marathon runners and controls at various bone sites

Region	All subjects			Male			Female		
	Amateur marathon	Control	P	Amateur marathon	Control	P	Amateur marathon	Control	P
Thoracic vertebrae	5.51 (4.46, 8.13)	4.93 (3.19, 5.68)	0.022	4.68 (4.15, 5.68)	3.57 (2.84, 5.18)	0.021	7.69 (6.23, 8.93)	5.87 (5.24, 7.35)	0.029
Lumbar vertebrae	5.10±1.64	3.68±1.48	0.001	4.49±1.38	3.01±1.02	<0.001	6.31±1.48	5.03±1.35	0.058
Sacrum	4.42 (3.37, 4.80)	2.98 (2.27, 3.78)	0.003	3.67±1.17	2.62±0.72	0.002	4.50 (4.27, 5.67)	4.46 (2.82, 5.43)	0.529
Hip	4.02±1.37	2.93±1.00	0.001	3.45±1.08	2.50±0.72	0.002	4.76 (4.42, 5.41)	3.92 (3.04, 4.34)	0.004

Data are presented as the mean ± standard deviation, or median (M) and quartile (Q1, Q3). SIR_{BM-muscle}, signal intensity ratio of bone marrow to muscle.

Table 3 Comparison of the ADC values ($\times 10^{-6}$ mm²/s) of bone marrow between the amateur marathon runners and controls at various bone sites

Region	All subjects			Male			Female		
	Amateur marathon	Control	P	Amateur marathon	Control	P	Amateur marathon	Control	P
Thoracic vertebrae	497.75±69.83	498.04±80.45	0.988	474.71 (448.00, 485.34)	472.09 (427.21, 491.33)	0.758	553.09±70.07	579.45±50.30	0.347
Lumbar vertebrae	531.41±65.43	515.69±90.45	0.444	508.27±55.77	476.83±77.61	0.149	577.68±60.50	593.42±59.81	0.566
Sacrum	574.67±48.66	546.03±78.11	0.094	569.89±49.02	523.81±77.25	0.03	584.21±49.04	590.47±61.38	0.804
Hip	592.69±51.24	525.02±99.03	0.002	577.36±42.06	481.16±87.29	<0.001	623.35±56.19	612.75±51.84	0.666

Data are presented as the mean ± standard deviation, or median (M) and quartile (Q1, Q3). ADC, apparent diffusion coefficient.

Table 4 Demographic characteristics of the DWI hyper- and hypo-intense male amateur marathon groups

Characteristic	Hypointense	Hyperintense	P value
Age (years)	41.6±5.211	41.40±6.00	0.937
The yearly running distance (km)	2,520±578.89	2,280±484.88	0.328
Running years (years)	6.00 (3.75, 7.75)	5.00 (3.38, 5.25)	0.247
BMI (kg/m ²)	23.88±1.20	23.95±2.31	0.933
WBC (10 ⁹ /L)	5.81±0.93	6.38±1.07	0.221
RDW-CV (%)	12.91±1.79	13.26±1.07	0.597
PLT (10 ⁹ /L)	218.44±60.87	192.4±45.14	0.291
RBC (10 ¹² /L)	4.82 (4.69, 5.17)	4.62 (4.55, 4.80)	0.123
HGB (g/L)	152.86 (142.75, 159.75)	143.00 (138.38, 154.50)	0.218

Data are presented as the mean ± standard deviation, or median (M) and quartile (Q1, Q3). DWI, diffusion-weighted imaging; BMI, body mass index; WBC, white blood cell; RDW-CV, red blood cell distribution width-coefficient of variation; PLT, platelet; RBC, red blood cell; HGB, hemoglobin.

CI: 0.834–0.923), and 0.930 (95% CI: 0.884–0.958), respectively]. The intra-observer reliability for the SI_{BM} , SI_{muscle} , ADC, and T2 measurements ranged from good to very good [ICC =0.938 (95% CI: 0.917–0.953), 0.733 (95% CI: 0.612–0.812), 0.865 (95% CI: 0.801–0.905), and 0.882 (95% CI: 0.770–0.936), respectively].

Discussion

In this study, we compared the WB-DWI bone marrow signal characteristics of 30 healthy adult amateur marathon runners (aged 30–50 years) with those of 30 healthy age- and gender-matched volunteers who had not engaged in any long-term sports training. The frequency difference of the bone marrow DWI ($b=800$ s/mm²) hyperintensity between the male amateur marathon runners and controls (50% *vs.* 5%) was much greater than that of the females (100% *vs.* 90%). These results indicate that marathon training increases the likelihood of bone marrow hyperintensity in DW images. Thus, when WB-DWI is used to screen bone marrow diseases, the patient's marathon training history should be considered to avoid false-positive diagnoses. The further signal quantitative study showed that the $SIR_{BM-muscle}$ values were significantly higher in the male amateur marathon runners than the male controls in the thoracic vertebrae (4.68 *vs.* 3.57), lumbar vertebrae (4.49 *vs.* 3.01), sacrum (3.67 *vs.* 2.62), and hip (3.45 *vs.* 2.50), which further supports the visual assessment results.

At birth, the entire skeleton is filled with red bone marrow, and the physiological conversion of red marrow into yellow marrow occurs with aging. The adult distribution of red bone marrow, which appears at age 25, is characterized by the presence of red bone marrow in the axial skeleton (vertebral bodies, sacral bone, and medial parts of hip bones) and articular ends of humeral and femoral bones (45,46). In this study, hypointensity was observed in the images of the humeral heads, femoral heads, and great trochanters of the 30 subjects who showed diffuse bone marrow hyperintensity in the DW images of the thoracolumbar vertebrae, sacrum, hips, ribs, sternum, and scapula (100%). Thus, we speculate that the bone marrow DWI hyperintensities caused by marathon training will not involve epiphyseal sites; however, further research is needed.

In the current study, 100% of the femoral metaphysis and proximal segments showed bone marrow DWI hyperintensity in the female amateur marathon runners,

compared with only 50% in the controls. Meanwhile, 60% of the humeral metaphysis and proximal segments showed hyperintensity in the female amateur marathon runners, compared with 40% in the controls. In the male amateur marathon runners, 30% of the femoral metaphysis and proximal segments showed hyperintensity, while the frequency for humeral metaphysis and proximal segments was 10% (compared to 0% in the controls for both). These results indicate that the change in bone marrow signal intensity caused by marathon training was more obvious in the femur than the humerus. We speculate that the increase in DWI bone marrow signal intensity might be related to the impact force on bones during marathon training, which explains why the signal change was much more pronounced in the femur than the humerus.

In our previous study, we found diffuse DWI hyperintensities of the bone marrow in 91% of premenopausal, 75% of perimenopausal, and 8% of postmenopausal women (32). In our current study, all the females were in the premenopausal period. The frequency of DWI bone marrow hyperintensity in the female controls was 90%, which is consistent with the findings of our previous study (32), while the frequency in the female marathon runners was 100%. There was no significant difference in the frequency between the female marathon runners and controls in the current study.

Fifty percent (10/20) of the male amateur marathon runners showed bone marrow DWI hyperintensity in current study. In our previous study (31), we found that only 3.3% of the males aged 21–50 years showed bone marrow DWI hyperintensity. These results indicate that marathon exercise increases the frequency of bone marrow high DWI signals; however, the reason for this needs to be further investigated.

Based on previous studies, bone marrow hyperintensity in DW images is related to the increased water content of the bone marrow, resulting from the T2 shine-through effect (31,32,47). In this study, the T2 values of the lumbar vertebrae were significantly higher in the male amateur marathon runners than the male controls (116.76 *vs.* 97.63 ms), which is consistent with the $SIR_{BM-muscle}$ results (see *Table 2*), which could be one reason for the increasing frequency of the high bone marrow DWI signal in male marathon runners. One reason for the increased water content of the bone marrow might be marrow hyperplasia stimulated by the impact force on bone created by long-term marathon training (31). No significant difference between the female amateur marathon runners and the

corresponding controls (118.58 vs. 124.10 ms) was found, which is similar to the $SIR_{BM-muscle}$ results (see *Table 2*). According to our previous study, the frequency of bone marrow DWI hyperintensity in reproductive-age women (91%) was higher than that in men (3.3%) (21–50 years old) (31,32), indicating that in reproductive-age women, menstruation and sex hormones could maintain red bone marrow status (48). There was no significant difference in the frequency of the bone marrow high DWI signal found between postmenopausal women (8%) and men aged 21–50 years (3.3%), $P=0.40$ (31,32), which may indicate that women's marrow transfers to yellow marrow after the loss of menstruation and sex hormones.

Finally, significant differences in the bone marrow ADC values between the amateur marathon runners and the controls were only observed in the male's sacrum (569.89×10^{-6} vs. 523.81×10^{-6} mm²/s) and hips (577.36×10^{-6} vs. 481.16×10^{-6} mm²/s) (see *Table 3*), which indicates that the ADC values are not important factors of the bone marrow high DWI signal. Further studies need to be conducted to clarify the underlying complex mechanism (49).

The current study had several limitations. First, the age range of the amateur marathon runners was narrow (30–50 years). Runners of other age ranges, particularly postmenopausal women, should be studied in future, as the bone marrow only shows a high signal visually in WB-DWI in 3.3–5.9% of 21–81 years old males (31) and 8% of postmenopausal women (32). If marathon training can increase the diffuse high signal frequency of bone marrow in DWI in other age ranges, further study is needed. Second, no histological analysis of bone marrow was performed. Third, the effects of other factors, such as the effect of running pace on the bone marrow DWI signal were not analyzed.

Conclusions

Marathon training resulted in bone marrow diffuse hyperintensity on WB-DWI, especially in male marathon runners. In the present study, bone marrow hyperintensity was observed in 50% of the male amateur marathon runners aged 30–50 years. However, bone marrow hyperintensity does not affect the humeral head, femoral head, and femoral trochanteric epiphysis. Our results suggest that when WB-DWI is used to screen bone marrow diseases, marathon training history should be considered to avoid false-positive diagnoses.

Acknowledgments

The authors would like to thank AiMi Academic Services (www.aimieditor.com) for their English language editing and review services. The authors would also like to thank Yongzhong Chen for his help in the image analysis process. *Funding:* This study was supported by the Science and Technology Program of Hebei Province (grant No. 22377751D to H.Y., and grant No. 223777112D to H.C.), and the Hebei Provincial Department of Finance (grant No. ZF2023074 to J.C.).

Footnote

Reporting Checklist: The authors have completed the STROBE reporting checklist. Available at <https://qims.amegroups.com/article/view/10.21037/qims-23-1006/rc>

Conflicts of Interest: All authors have completed the ICMJE uniform disclosure form (available at <https://qims.amegroups.com/article/view/10.21037/qims-23-1006/coif>). H.Y. reports that this study was supported by the Science and Technology Program of Hebei Province (grant No. 22377751D). H.C. reports that this study was supported by the Science and Technology Program of Hebei Province (grant No. 223777112D). J.C. reports that this study was supported by the Hebei Provincial Department of Finance (grant No. ZF2023074). The other authors have no conflicts of interest to declare.

Ethical Statement: The authors are accountable for all aspects of the work in ensuring that questions related to the accuracy or integrity of any part of the work are appropriately investigated and resolved. This study was conducted in accordance with the Declaration of Helsinki (as revised in 2013) and was approved by the Ethics Committee of The Third Hospital of Hebei Medical University. Individual consent of each participant was obtained.

Open Access Statement: This is an Open Access article distributed in accordance with the Creative Commons Attribution-NonCommercial-NoDerivs 4.0 International License (CC BY-NC-ND 4.0), which permits the non-commercial replication and distribution of the article with the strict proviso that no changes or edits are made and the original work is properly cited (including links to both the formal publication through the relevant DOI and the license). See: <https://creativecommons.org/licenses/by-nc-nd/4.0/>.

References

1. Takahara T, Imai Y, Yamashita T, Yasuda S, Nasu S, Van Cauteren M. Diffusion weighted whole body imaging with background body signal suppression (DWIBS): technical improvement using free breathing, STIR and high resolution 3D display. *Radiat Med* 2004;22:275-82.
2. Mesguich C, Hulin C, Latrabe V, Lascaux A, Bordenave L, Hindié E, Marit G. Prospective comparison of 18-FDG PET/CT and whole-body diffusion-weighted MRI in the assessment of multiple myeloma. *Ann Hematol* 2020;99:2869-80.
3. Sun W, Li M, Gu Y, Sun Z, Qiu Z, Zhou Y. Diagnostic Value of Whole-Body DWI With Background Body Suppression Plus Calculation of Apparent Diffusion Coefficient at 3 T Versus (18)F-FDG PET/CT for Detection of Bone Metastases. *AJR Am J Roentgenol* 2020;214:446-54.
4. Daldrup-Link HE, Franzius C, Link TM, Laukamp D, Sciuk J, Jürgens H, Schober O, Rummeny EJ. Whole-body MR imaging for detection of bone metastases in children and young adults: comparison with skeletal scintigraphy and FDG PET. *AJR Am J Roentgenol* 2001;177:229-36.
5. Sakurai Y, Kawai H, Iwano S, Ito S, Ogawa H, Naganawa S. Supplemental value of diffusion-weighted whole-body imaging with background body signal suppression (DWIBS) technique to whole-body magnetic resonance imaging in detection of bone metastases from thyroid cancer. *J Med Imaging Radiat Oncol* 2013;57:297-305.
6. Zugni F, Padhani AR, Koh DM, Summers PE, Bellomi M, Petralia G. Whole-body magnetic resonance imaging (WB-MRI) for cancer screening in asymptomatic subjects of the general population: review and recommendations. *Cancer Imaging* 2020;20:34.
7. Greer MC, Voss SD, States LJ. Pediatric Cancer Predisposition Imaging: Focus on Whole-Body MRI. *Clin Cancer Res* 2017;23:e6-e13.
8. Barnes A, Alonzi R, Blackledge M, Charles-Edwards G, Collins DJ, Cook G, et al. UK quantitative WB-DWI technical workgroup: consensus meeting recommendations on optimisation, quality control, processing and analysis of quantitative whole-body diffusion-weighted imaging for cancer. *Br J Radiol* 2018;91:20170577.
9. Petralia G, Koh DM, Attariwala R, Busch JJ, Eeles R, Karow D, Lo GG, Messiou C, Sala E, Vargas HA, Zugni F, Padhani AR. Oncologically Relevant Findings Reporting and Data System (ONCO-RADS): Guidelines for the Acquisition, Interpretation, and Reporting of Whole-Body MRI for Cancer Screening. *Radiology* 2021;299:494-507.
10. Messiou C, Hillengass J, Delorme S, Lecouvet FE, Mouloupoulos LA, Collins DJ, Blackledge MD, Abildgaard N, Østergaard B, Schlemmer HP, Landgren O, Asmussen JT, Kaiser MF, Padhani A. Guidelines for Acquisition, Interpretation, and Reporting of Whole-Body MRI in Myeloma: Myeloma Response Assessment and Diagnosis System (MY-RADS). *Radiology* 2019;291:5-13.
11. Padhani AR, Lecouvet FE, Tunariu N, Koh DM, De Keyzer F, Collins DJ, Sala E, Schlemmer HP, Petralia G, Vargas HA, Fanti S, Tombal HB, de Bono J. METastasis Reporting and Data System for Prostate Cancer: Practical Guidelines for Acquisition, Interpretation, and Reporting of Whole-body Magnetic Resonance Imaging-based Evaluations of Multiorgan Involvement in Advanced Prostate Cancer. *Eur Urol* 2017;71:81-92.
12. Lee K, Park HY, Kim KW, Lee AJ, Yoon MA, Chae EJ, Lee JH, Chung HW. Advances in whole body MRI for musculoskeletal imaging: Diffusion-weighted imaging. *J Clin Orthop Trauma* 2019;10:680-6.
13. Sung H, Ferlay J, Siegel RL, Laversanne M, Soerjomataram I, Jemal A, Bray F. Global Cancer Statistics 2020: GLOBOCAN Estimates of Incidence and Mortality Worldwide for 36 Cancers in 185 Countries. *CA Cancer J Clin* 2021;71:209-49.
14. Awolaran O, Brooks SA, Lavender V. Breast cancer osteomimicry and its role in bone specific metastasis; an integrative, systematic review of preclinical evidence. *Breast* 2016;30:156-71.
15. Bevers TB, Niell BL, Baker JL, Bennett DL, Bonaccio E, Camp MS, et al. NCCN Guidelines® Insights: Breast Cancer Screening and Diagnosis, Version 1.2023. *J Natl Compr Canc Netw* 2023;21:900-9.
16. Choi JE, Kim Z, Park CS, Park EH, Lee SB, Lee SK, Choi YJ, Han J, Jung KW, Kim HJ, Kim HA; . Breast Cancer Statistics in Korea, 2019. *J Breast Cancer* 2023;26:207-20.
17. Shinden Y, Sugimachi K, Tanaka F, Fujiyoshi K, Kijima Y, Natsugoe S, Mimori K. Clinicopathological characteristics of disseminated carcinomatosis of the bone marrow in breast cancer patients. *Mol Clin Oncol* 2018;8:93-8.
18. Ak I, Sivrikoz MC, Entok E, Vardareli E. Discordant findings in patients with non-small-cell lung cancer: absolutely normal bone scans versus disseminated bone metastases on positron-emission tomography/computed tomography. *Eur J Cardiothorac Surg* 2010;37:792-6.
19. Zhou M, Chen Y, Liu J, Huang G. A predicting model of bone marrow malignant infiltration in (18)F-FDG PET/

- CT images with increased diffuse bone marrow FDG uptake. *J Cancer* 2018;9:1737-44.
20. Tanguay M, Dagenais C, LeBlanc R, Ahmad I, Claveau JS, Roy J. Young Myeloma Patients: A Systematic Review of Manifestations and Outcomes. *Curr Oncol* 2023;30:5214-26.
 21. Sun M, Cheng J, Ren C, Zhang Y, Li Y, Wang L, Liu Y. Differentiation of Diffuse Infiltration Pattern in Multiple Myeloma From Hyperplastic Hematopoietic Bone Marrow: Qualitative and Quantitative Analysis Using Whole-Body MRI. *J Magn Reson Imaging* 2022;55:1213-25.
 22. Du M, Chen W, Liu K, Wang L, Hu Y, Mao Y, Sun X, Luo Y, Shi J, Shao K, Huang H, Ye D. The Global Burden of Leukemia and Its Attributable Factors in 204 Countries and Territories: Findings from the Global Burden of Disease 2019 Study and Projections to 2030. *J Oncol* 2022;2022:1612702.
 23. Han T, Barcos M, Emrich L, Ozer H, Gajera R, Gomez GA, Reese PA, Minowada J, Bloom ML, Sadamori N. Bone marrow infiltration patterns and their prognostic significance in chronic lymphocytic leukemia: correlations with clinical, immunologic, phenotypic, and cytogenetic data. *J Clin Oncol* 1984;2:562-70.
 24. Yang SJ, Yang F, Gao Y, Su YF, Sun W, Jia SW, Wang Y, Lam WK. Gender and Age Differences in Performance of Over 70,000 Chinese Finishers in the Half- and Full-Marathon Events. *Int J Environ Res Public Health* 2022;19:7802.
 25. Nakanishi K, Tanaka J, Nakaya Y, Maeda N, Sakamoto A, Nakayama A, Satomura H, Sakai M, Konishi K, Yamamoto Y, Nagahara A, Nishimura K, Takenaka S, Tomiyama N. Whole-body MRI: detecting bone metastases from prostate cancer. *Jpn J Radiol* 2022;40:229-44.
 26. Cao W, Liang C, Gen Y, Wang C, Zhao C, Sun L. Role of diffusion-weighted imaging for detecting bone marrow infiltration in skull in children with acute lymphoblastic leukemia. *Diagn Interv Radiol* 2016;22:580-6.
 27. Sun M, Cheng J, Zhang Y, Wang F, Meng Y, Fu X. Application value of diffusion weighted whole body imaging with background body signal suppression in monitoring the response to treatment of bone marrow involvement in lymphoma. *J Magn Reson Imaging* 2016;44:1522-9.
 28. Attariwala R, Picker W. Whole body MRI: improved lesion detection and characterization with diffusion weighted techniques. *J Magn Reson Imaging* 2013;38:253-68.
 29. Chen YY, Wu CL, Shen SH. High Signal in Bone Marrow on Diffusion-Weighted Imaging of Female Pelvis: Correlation With Anemia and Fibroid-Associated Symptoms. *J Magn Reson Imaging* 2018;48:1024-33.
 30. Ording Müller LS, Avenarius D, Olsen OE. High signal in bone marrow at diffusion-weighted imaging with body background suppression (DWIBS) in healthy children. *Pediatr Radiol* 2011;41:221-6.
 31. Cui FZ, Cui JL, Wang SL, Yu H, Sun YC, Zhao N, Cui SJ. Signal characteristics of normal adult bone marrow in whole-body diffusion-weighted imaging. *Acta Radiol* 2016;57:1230-7.
 32. Cui FZ, Yao QQ, Cui JL, Wei W, Duan LS, Yu H. The signal intensity characteristics of normal bone marrow in diffusion weighted imaging at various menstrual status women. *Eur J Radiol* 2021;143:109938.
 33. Bao H, He X, Li X, Cao Y, Zhang N. Magnetic resonance imaging study of normal cranial bone marrow conversion at high altitude. *Quant Imaging Med Surg* 2022;12:3126-37.
 34. Althoefer C, Bertz H, Ghanem NA, Langer M. Extent and time course of morphological changes of bone marrow induced by granulocyte-colony stimulating factor as assessed by magnetic resonance imaging of healthy blood stem cell donors. *J Magn Reson Imaging* 2001;14:141-6.
 35. Shigematsu Y, Hirai T, Kawanaka K, Shiraishi S, Yoshida M, Kitajima M, Uetani H, Azuma M, Iryo Y, Yamashita Y. Distinguishing imaging features between spinal hyperplastic hematopoietic bone marrow and bone metastasis. *AJNR Am J Neuroradiol* 2014;35:2013-20.
 36. Shellock FG, Morris E, Deutsch AL, Mink JH, Kerr R, Boden SD. Hematopoietic bone marrow hyperplasia: high prevalence on MR images of the knee in asymptomatic marathon runners. *AJR Am J Roentgenol* 1992;158:335-8.
 37. Althoefer C, Schmid A, Büchert M, Ghanem NA, Heinrich L, Langer M. Characterization of hematopoietic bone marrow in male professional cyclists by magnetic resonance imaging of the lumbar spine. *J Magn Reson Imaging* 2002;16:284-8.
 38. Caldemeyer KS, Smith RR, Harris A, Williams T, Huang Y, Eckert GJ, Slemenda CW. Hematopoietic bone marrow hyperplasia: correlation of spinal MR findings, hematologic parameters, and bone mineral density in endurance athletes. *Radiology* 1996;198:503-8.
 39. Zhang Y, Shu D, Yao W, Ding J, Chen L, Lin X, Tian T, Liu J. MRI study of changes in knee bone marrow edema-like signal in asymptomatic amateur marathon runners before and after half-marathon running. *Clin Imaging* 2021;80:150-7.

40. Liu Y, Chen Y, Han P, Ma W, Cai M, Wang F, Wang J, Zhang J, He W, Zhu X, Guo Q, Yu Y. Combined effect of obesity and low physical performance on the incidence of hypertension in Chinese community-dwelling older population. *J Hum Hypertens* 2021;35:970-7.
41. Padhani AR, van Ree K, Collins DJ, D'Sa S, Makris A. Assessing the relation between bone marrow signal intensity and apparent diffusion coefficient in diffusion-weighted MRI. *AJR Am J Roentgenol* 2013;200:163-70.
42. Laborie LB, Lehmann TG, Engesaeter IØ, Eastwood DM, Engesaeter LB, Rosendahl K. Prevalence of radiographic findings thought to be associated with femoroacetabular impingement in a population-based cohort of 2081 healthy young adults. *Radiology* 2011;260:494-502.
43. Landis JR, Koch GG. The measurement of observer agreement for categorical data. *Biometrics* 1977;33:159-74.
44. Park S, Kwack KS, Chung NS, Hwang J, Lee HY, Kim JH. Intravoxel incoherent motion diffusion-weighted magnetic resonance imaging of focal vertebral bone marrow lesions: initial experience of the differentiation of nodular hyperplastic hematopoietic bone marrow from malignant lesions. *Skeletal Radiol* 2017;46:675-83.
45. Małkiewicz A, Dziedzic M. Bone marrow reconversion - imaging of physiological changes in bone marrow. *Pol J Radiol* 2012;77:45-50.
46. Chan BY, Gill KG, Rebsamen SL, Nguyen JC. MR Imaging of Pediatric Bone Marrow. *Radiographics* 2016;36:1911-30.
47. Wáng YXJ, Aparisi Gómez MP, Ruiz Santiago F, Bazzocchi A. The relevance of T2 relaxation time in interpreting MRI apparent diffusion coefficient (ADC) map for musculoskeletal structures. *Quant Imaging Med Surg* 2023;13:7657-66.
48. Chen WT, Shih TT, Chen RC, Lo SY, Chou CT, Lee JM, Tu HY. Vertebral bone marrow perfusion evaluated with dynamic contrast-enhanced MR imaging: significance of aging and sex. *Radiology* 2001;220:213-8.
49. Wáng YXJ, Ma FZ. A tri-phasic relationship between T2 relaxation time and magnetic resonance imaging (MRI)-derived apparent diffusion coefficient (ADC). *Quant Imaging Med Surg* 2023;13:8873-80.

Cite this article as: Cao H, Cui F, Yu H, Cui J, Ma F, Duan L. Normal bone marrow signal characteristics in whole-body diffusion-weighted images of amateur marathon runners. *Quant Imaging Med Surg* 2024;14(3):2321-2333. doi: 10.21037/qims-23-1006